Comparison of Radiographs and Computed Tomography for the Screening of Anterior Inferior Iliac Spine Impingement

Broc R. Schindler, B.S., Melanie B. Venderley, B.S., Jacob D. Mikula, B.S., Jorge Chahla, M.D., Grant J. Dornan, M.S., Travis Lee Turnbull, Ph.D., Robert F. LaPrade, M.D., Ph.D., and Marc J. Philippon, M.D.

Purpose: To compare radiographic and 3-dimensional (3D) computed tomography (CT) imaging modalities for the screening of anterior inferior iliac spine (AIIS) impingement by establishing imaging measurement related to the AIIS. **Methods:** Anteroposterior and false-profile radiographs and 3D CT scans were obtained on 10 human cadaveric pelvises. On the anteroposterior view for each methodology, 2 measurements were calculated: distance to the most lateral AIIS from the 12 o'clock position on the acetabular rim, and the angle between the lateral AIIS and the sagittal plane. On the false-profile view for each methodology, 2 measurements were calculated: distance to the anterior AIIS from the 12 o'clock position on the acetabular rim, and the angle between the anterior AIIS and the sagittal plane. Inter-rater and intrarater reliability analyses were performed for both methods in addition to an intermethod analysis. **Results:** The radiographic false-profile view was the most repeatable orientation, with intraclass correlation coefficients showing excellent reproducibility in both inter-rater (angle: 0.980, distance: 0.883) and intrarater (angle: 0.995, distance: 0.995) analyses. The mean distance from the 12 o'clock position of the acetabular rim to the most anterior/lateral aspect of the AIIS was 41.4 mm and 16.0 mm on the radiographic false-profile and anteroposterior views, respectively. Intermethod analysis showed a systematic, quantitative bias between modalities (anteroposterior view: −4.1 mm, 6.7°; false-profile view: −0.1 mm, 8.3°), which will remain relatively consistent as evidenced by the strong individual reproducibility of each measurement. **Conclusions:** AIIS morphology in relation to the acetabular rim 12 o'clock position and its angle relative to the sagittal plane can be quantitatively determined using either radiographic or 3D CT imaging modalities. **Clinical Relevance:** Radiographic evaluation may be a valuable tool in the screening of AIIS impingement.

Although computed tomography (CT) offers many advantages in the preoperative planning of cases that involve the correction of bony deformities, it has been reported that obtaining one CT image of the hip delivers the equivalent radiation dose of receiving 39 conventional chest radiographs.[1] Because plain radiographs are the first imaging modality indicated for the evaluation of hip pathologies,[2] establishing radiographic protocols that are equivalent to CT assessments for pathologies could drastically limit radiation exposure to patients during the evaluation process.

In recent years, studies have been conducted to compare diagnostic measurements related to femoroacetabular impingement (FAI) obtained using CT and radiographic modalities.[3-5] However, there is a paucity of available literature for the anterior inferior iliac spine (AIIS), which is increasingly recognized as a site related to extra-articular hip pathologies.[6-14]

To date, the normal[15] and potentially pathologic[7,8] morphology of the AIIS have been described using 2-dimensional (2D) and 3-dimensional (3D) CT, respectively. Amar et al.[15] used 2D CT to describe the normal morphology of the AIIS based on the size, location, and position of the AIIS with respect to patient size and sex. Similarly, Hetsroni et al.[9] developed a 3D CT qualitative method to describe a potentially pathologic AIIS morphology in a symptomatic FAI

From the Department of BioMedical Engineering, Steadman Philippon Research Institute (B.R.S., M.B.V., J.D.M., J.C., G.J.D., T.L.T., R.F.L., M.J.P.); and The Steadman Clinic (R.F.L., M.J.P.), Vail, Colorado, U.S.A.

The authors report the following potential conflict of interest or source of funding: R.F.L. and M.J.P. receive support from Arthrex; Ossur; Siemans; Smith & Nephew; Health East, Norway; and NIH R-13 grant for biologics.

Received June 7, 2016; accepted October 20, 2016.

Address correspondence to Marc J. Philippon, M.D., Steadman Philippon Research Institute, 181 W. Meadow Drive, Suite 400, Vail, CO 81657, U.S.A. E-mail: m@mjphilippon.com

0749-8063/16495/$36.00

http://dx.doi.org/10.1016/j.arthro.2016.10.018

population. In addition, using radiographs, Lee et al.[16] have quantitatively described the location of the AIIS on anteroposterior (AP) radiographs by measuring the distance from the AIIS to a reference line drawn through the acetabular teardrop. This measurement provides a vertical approximation to the location of the AIIS; however, it does not address its location medially and/or laterally along that reference line. Because none of these aforementioned studies related their CT or radiographic findings to one another, a need exists to compare radiographic and 3D CT measurements related to the AIIS to determine whether radiographs are a valid methodology for the evaluation of AIIS-involved extra-articular hip pathologies.

The purpose of this study was to compare radiographic and 3D CT imaging modalities for the screening of AIIS impingement by establishing imaging measurement related to the AIIS. We hypothesized that a high correlation would exist between measurements obtained using either radiographic or CT imaging modalities.

Methods

Cadaveric Specimens

Ten human fresh-frozen pelvises with full femurs (mean age: 57.7 years; range: 45-69; males: 7; females: 3) were obtained and used from concurrent radiographic imaging studies.[17] Each specimen contained radio-opaque hardware (metallic spheres) placed at anatomical landmarks of interest (e.g., the AIIS) on one side of the pelvis (the "symptomatic side"), providing verification that the measurements related to the AIIS were consistently and correctly performed. Furthermore, the use of radio-opaque markers precluded potential partial volume effects in CT images by providing a readily identifiable feature at the exact location of each anatomical landmark.

Image Collection

Standard clinical radiographs of the pelvis were obtained in AP and false-profile views by mounting the specimen to an alignment fixture.[16] After the pelvis was mounted, a true AP image was achieved by verifying that the obturator foramina were symmetrical, the ilioischial line was just medial to the acetabular fossa, and the superior border of the pubic symphysis was approximately 32 mm distal to the sacrococcygeal joint in male specimens and approximately 47 mm in female specimens.[18-20] False-profile positioning was achieved using a custom jig that tilted the platform to 65° of inclination, such that the hip containing the metallic spheres (which would be considered the symptomatic hip in the clinical setting) was closer to the cassette. In addition, for the false-profile view, the femur was removed on the side of the hip with metallic spheres to simplify the imaging and measurement procedures.

To provide a frame of reference and account for fluctuations in magnification due to varying distances from the x-ray source, a 25.4-mm-diameter stainless steel sphere (tolerance ± 0.00254 mm, sphericity: 0.00061 mm, Small Parts, Logansport, IN) was included in the field of view, set at the level of the anatomic landmarks to be measured via a custom adjustable height fixture.

After radiographic imaging of each specimen, clinical-grade CT scans of each pelvis were acquired (Aquilion Premium; Toshiba America Medical Systems, Tustin, CA) at a 0.5 mm slice thickness, 120 kVp voltage, 150 mA current, and 750 ms exposure time, using a helical scan. Mimics (Materialise, Leuven, Belgium) computational modeling software was then used to create a 3D bone model from the CT data. This model allowed for quantitative measurements of the AIIS to be made and subsequent comparison with radiographic measurements.

Radiographic Measurements

All radiographic measurements were calculated using a digital picture archiving and communication system (OrthoCase, Merge Healthcare, Chicago, IL). Angle measurements made on the AP view were assessed bilaterally (n = 20), with the metallic sphere on the symptomatic side as a reference for the AIIS on the contralateral, unmarked hip. The AP distance measurement and false-profile view measurements were made only relative to the hip that contained the metallic spheres (n = 10). On the AP view, the distance from the 12 o'clock position on the acetabular rim (marked by a metallic sphere) to the lateral aspect of the AIIS was measured. In addition, a variation of the lateral center-edge angle[18] was drawn with 2 distinct differences. First, the vertical line was constructed through the center of the acetabulum, instead of the center of the femoral head, which was found by drawing a circle along the rim. Second, the angle was constructed by referencing the most lateral aspect of the AIIS instead of the lateral sourcil. The most lateral aspect of the AIIS was determined by moving immediately lateral along the axial plane from a metallic sphere that had been placed at the anterior-most aspect of the center of the origin of the rectus femoris muscle. These 2 measurements assisted in describing any lateral morphology changes to the AIIS. All reference lines and metallic sphere landmarks for the AP radiograph are depicted in Figure 1A and the resulting measurements are shown in Figure 1B.

On the false-profile view, the distance from the 12 o'clock position on the acetabular rim (marked by a metallic sphere) to the most anterior aspect of the AIIS was measured. In addition, a variation of the anterior center-edge angle[18] was drawn with 2 distinct differences. First, the vertical line was constructed through the center of the acetabulum, instead of the center of the femoral head, which was found by drawing a circle

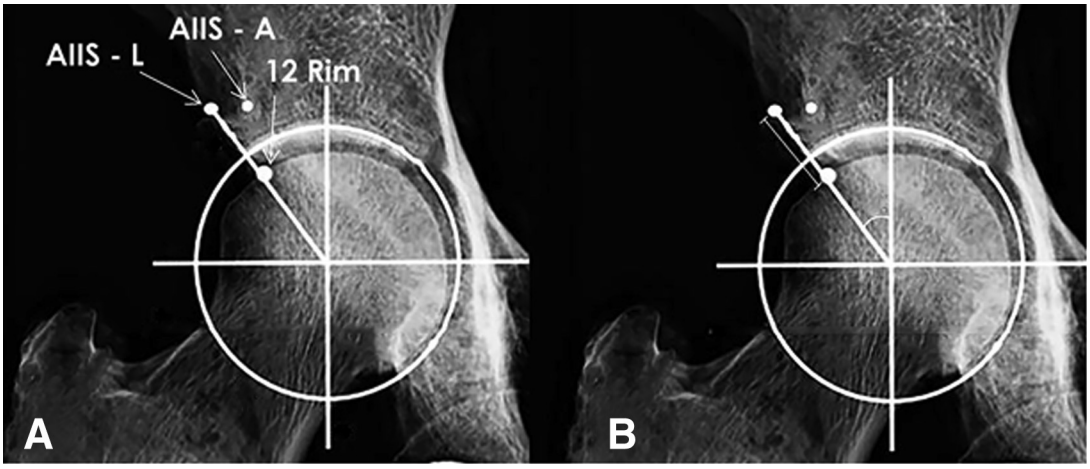

Fig 1. Anteroposterior (AP) reference lines and measurements on a right hip. (A) The reference lines and points made in the radiographic AP view (12 Rim, the 12 o'clock position on the rim of the ipsilateral acetabulum; AIIS-A, most anterior location of the anterior inferior iliac spine; AIIS-L, most lateral location of the anterior inferior iliac spine). (B) Two measurements made with respect to these references.

along the rim. Second, the angle was constructed by referencing the most anterior aspect of the AIIS (marked by a metallic sphere) instead of the anterior sourcil. These 2 measurements assisted in describing any anterior or inferior morphology changes to the AIIS. All reference lines and metallic sphere landmarks for the false-profile radiograph are depicted in Figure 2A and the resulting measurements are shown in Figure 2B.

CT Measurements

Using computational modeling software (Mimics, Materialise), 3D coordinate points denoting 6 anatomic landmarks (bilateral anterior superior iliac spine [ASIS], ipsilateral posterior superior iliac spine [PSIS], the 12 o'clock position on the rim of the ipsilateral acetabulum, and the most anterior and lateral aspects of the ipsilateral AIIS) relative to the "symptomatic" hip containing the metallic spheres were identified by an orthopaedic surgeon (J.C.) and recorded for each CT. The center of the ipsilateral acetabulum was also obtained by creating a sphere within the acetabulum (Fig 3). Before the measurements were performed, an orthopaedic surgeon (J.C.) reviewed each specimen using the classification system developed by Hetsroni et al.[9]

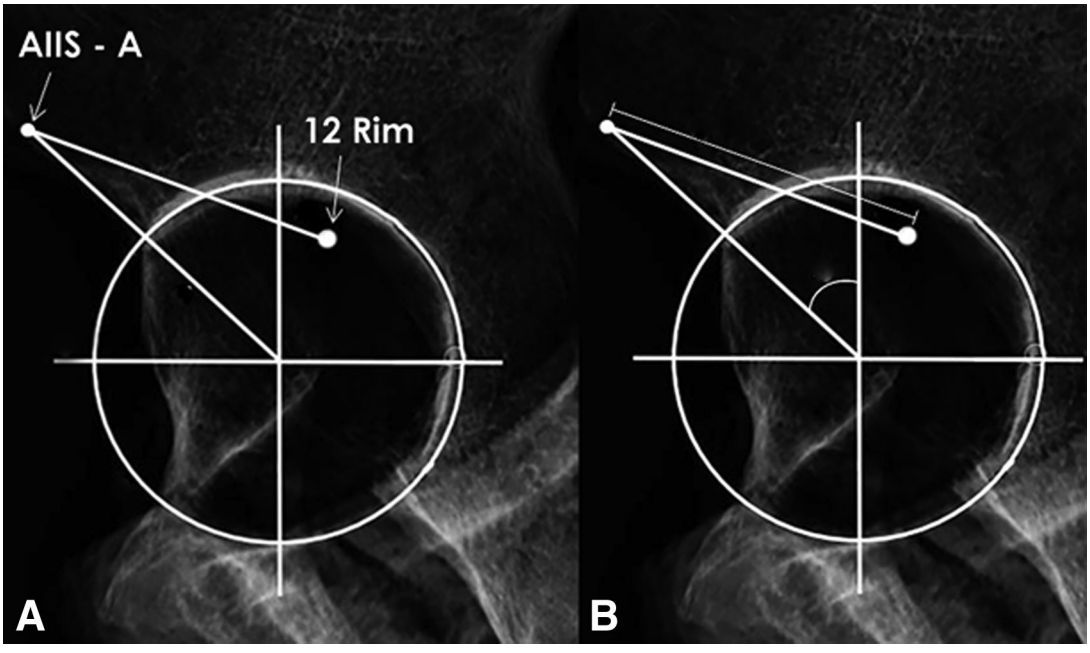

Fig 2. False-profile (FP) reference lines and measurements on a right hip. (A) The reference lines and points made in the radiographic FP view (12 Rim, the 12 o'clock position on the rim of the ipsilateral acetabulum; AIIS-A, most anterior location of the anterior inferior iliac spine). (B) Two measurements made with respect to these references.

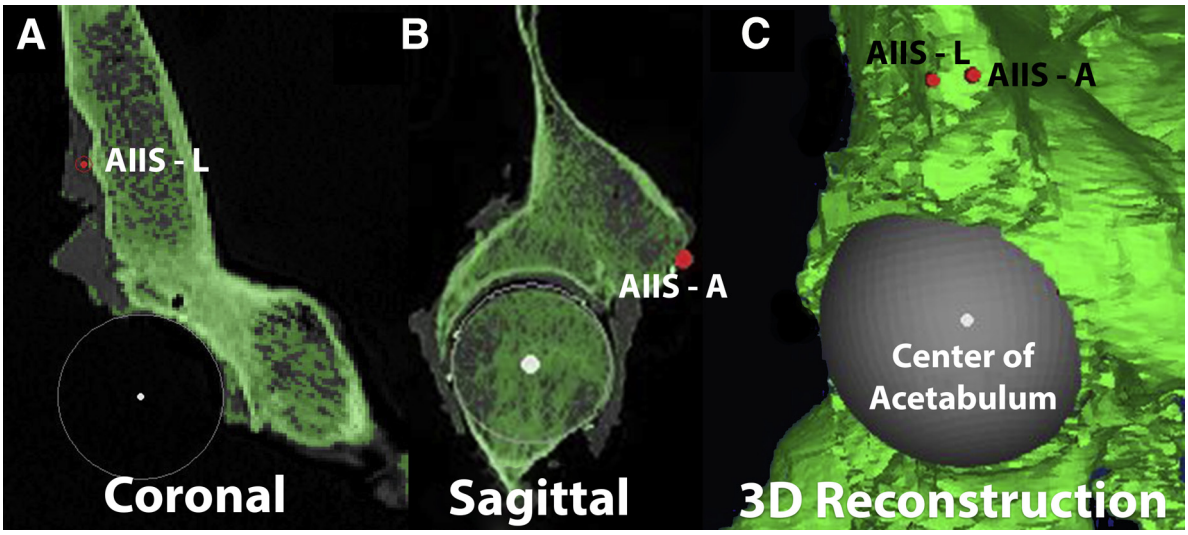

Fig 3. Pelvic 3D CT reconstruction of a right hip. (A, B) The 3D points representing the AIIS-L and the center of the femoral head on 2D CT slices, which correspond to the radiographic images in Figures 1A and 2A, respectively. The 2D coordinates of these locations were then subsequently used to make the same measurements developed in Figures 1B and 2B, so a comparison between methodologies could be determined. (C) The plotted 3D CT points demarcating the AIIS-A, AIIS-L, and the center of the acetabulum using Mimics software. (3D, 3-dimensional; AIIS-A, most anterior location of the anterior inferior iliac spine; AIIS-L, most lateral location of anterior inferior iliac spine; CT, computed tomography.)

The 3D coordinates defining the ASIS and PSIS locations were used in a custom Matlab script (Mathworks, Natick, MA) to orient each pelvis to a normalized position in accordance with the International Society of Biomechanics joint coordinate system recommendations.[21] Using these International Society of Biomechanics standards, a new, local coordinate reference frame was developed for each pelvis to make anatomically correct measurements that could be compared with other specimens regardless of the initial pelvis orientation.

Once anatomically oriented, predefined coordinates (e.g., Fig 3C) were used to computationally calculate 2D measurements within Matlab. On the AP view, a 2D distance was computed from the 12 o'clock acetabular rim position to the most lateral AIIS (Fig 3A). In addition, a 2D angle was calculated between the most lateral AIIS and the sagittal plane (Fig 3A). These measurements correspond to the radiographic measurements shown in Figure 1B. Each pelvis was then computationally rotated to obtain a false-profile view.[22] A 2D distance measurement from the 12 o'clock acetabular rim position to the anterior AIIS, followed by a 2D angle measurement between the anterior AIIS and the sagittal plane, was calculated (Fig 3B). These measurements correspond to the radiographic measurements shown in Figure 2B.

Statistical Analysis

Each measurement was summarized by the mean and standard deviation among the specimens. To assess measurement repeatability, all measurements were performed by 3 investigators (B.R.S., J.D.M., J.C.). Two weeks after the initial set of measurements were made one investigator (J.D.M.) performed a second round of measurements. Inter-rater and intrarater reliability were assessed for each measurement and imaging modality. Intermethod reliability was also assessed as the agreement between radiographic and 3D CT measurements. In each case, a 2-way random effects model was used to calculate the single measures, absolute agreement version of the intraclass correlation coefficient (ICC). A nonparametric 95% bootstrap confidence interval was reported with each ICC calculation. To further assess the intermethod reliability, Bland-Altman 95% limit of agreement analyses were performed. This tool aids in clinical interpretation by determining the bias (average measurement difference between raters, rounds, or methods) and spread of the observed differences between radiographic and 3D CT measurements in the units of the measurement. The ICC values were interpreted as follows: ICC <0.40 = poor agreement, $0.4 \leq$ ICC <0.75 = fair to good agreement, ICC ≥ 0.75 = excellent agreement.[23] All statistical analyses were performed with the statistical package R (R Development Core Team, Vienna, Austria, with packages *psy* and *boot*).

Results

Specimen Classification

No specimens exhibited a significant type 3 morphological AIIS variant.[9]

Intramethod Analyses: Distance Measurements

Generally, the radiographic false-profile view was the most repeatable orientation for distance

Table 1. Intramethod Analyses (Inter-rater and Intrarater Reliability Analyses) for Each Imaging Modality

					Inter-rater			Intrarater		
		n	Mean	SD	Agreement ICC	95% CI LB	95% CI UB	Agreement ICC	95% CI LB	95% CI UB
AP distance*	XR	10	16.0	3.24	0.838	0.639	0.934	0.980	0.936	0.994
	CT	10	20.5	3.80	0.521	0.284	0.745	0.667	0.304	0.915
False-profile distance†	XR	10	41.4	5.86	0.883	0.514	0.985	0.995	0.960	1.000
	CT	10	41.5	3.60	0.783	0.521	0.882	0.787	0.585	0.921
AP angle‡	XR	20	34.2	7.50	0.914	0.723	0.968	0.962	0.860	0.990
	CT	20	27.3	7.72	0.806	0.550	0.936	0.983	0.933	0.996
False-profile angle§	XR	10	51.0	5.98	0.980	0.949	0.993	0.995	0.988	0.997
	CT	10	42.9	5.28	0.835	0.399	0.964	0.771	0.148	0.935

AIIS, anterior inferior iliac spine; AP, anteroposterior; CI, confidence interval; CT, computed tomography; ICC, intraclass correlation coefficients; LB, lower bound; n, number of measurements; SD, standard deviation; UB, upper bound; XR, x-ray.
*AP distance: distance (mm) to the most lateral AIIS from the 12 o'clock position on the acetabular rim.
†False-profile distance: distance (mm) to the anterior AIIS from the 12 o'clock position on the acetabular rim.
‡AP angle: angle (°) between the most lateral AIIS and the sagittal plane.
§False-profile angle: angle (°) between the anterior AIIS and the sagittal plane.

measurements, with the ICCs showing excellent reproducibility in both inter-rater (0.883) and intrarater (0.995) analyses. On the false-profile view, the mean distance from the 12 o'clock position of the acetabular rim to the most anterior aspect of the AIIS was 41.4 mm on radiographs and 41.5 mm on 3D CT. On the AP view, the mean distance from the 12 o'clock position on the acetabular rim to the most lateral aspect of the AIIS was 16.0 mm on radiographs and 20.5 mm on 3D CT. For each measurement calculated, except for the 3D CT distance from the 12 o'clock position on the acetabular rim to the AIIS measured in the AP view, the inter-rater and intrarater reliability analysis showed excellent reproducibility on both radiographs and 3D CT (Table 1).

Intramethod Analyses: Angle Measurements

Generally, the radiographic false-profile view was the most repeatable orientation for angle measurements, with the ICCs showing excellent reproducibility in both inter-rater (0.980) and intrarater (0.995) analyses. On the false-profile view, the mean angle between the most anterior aspect of the AIIS and the sagittal plane was 51.0° on radiographs and 42.9° on 3D CT. On the AP view, the mean angle between the most lateral aspect of the AIIS and the sagittal plane was 34.2° on radiographs and 27.3° on 3D CT. For each measurement calculated, the inter-rater and intrarater reliability analysis showed excellent reproducibility on both radiographs and 3D CT (Table 1).

Intermethod Analysis: Distance and Angle Measurements

For the distance intermethod reliability, the ICCs showed poor reproducibility for distances measured on the AP view (0.332) and fair reproducibility for distances measured on the false-profile view (0.443) with a bias of −4.1 mm and −0.1 mm, respectively. For the angle intermethod reliability, the ICCs indicated good agreement for angles measured on the AP view (0.638) and poor agreement for angles measured on the false-profile view (0.180) with systematic biases of 6.7° and 8.3°, respectively (Table 2).

Discussion

The most important finding of this study was that the newly proposed quantitative measurements related to the AIIS (direct distances and angles) had strong reproducibility for both radiographic and 3D CT imaging modalities, individually. Specifically, the false-profile radiographic view was the most accurate and reproducible view to show AIIS morphology when using distance and angle measurements. Furthermore, using the center of the acetabulum, instead of the center of the femoral head (as with the standard center-edge angles), is even more clinically applicable because

Table 2. Intermethod Reliability Analysis Comparing Imaging Modalities (Radiographs to 3-Dimensional CT)

	n	Agreement ICC	95% CI LB	95% CI UB	Bias	Lower LOA	Upper LOA
AP distance*	10	0.322	−0.028	0.623	−4.1	−10.5	2.4
False-profile distance†	10	0.443	0.119	0.681	−0.1	−10.6	10.4
AP angle‡	20	0.638	0.379	0.832	6.7	−0.7	14.2
False-profile angle§	10	0.180	−0.120	0.606	8.3	−3.8	20.4

AIIS, anterior inferior iliac spine; AP, anteroposterior; CI, confidence interval; CT, computed tomography; ICC, intraclass correlation coefficients; LB, lower bound; LOA, limit of agreement; n, number of measurements; SD, standard deviation; UB, upper bound.
*AP distance: distance (mm) to the most lateral AIIS from the 12 o'clock position on the acetabular rim.
†False-profile distance: distance (mm) to the anterior AIIS from the 12 o'clock position on the acetabular rim.
‡AP angle: angle (°) between the most lateral AIIS and the sagittal plane.
§False-profile angle: angle (°) between the anterior AIIS and the sagittal plane.

narrowing of the femoroacetabular joint space will not affect the measurements. Finally, a systematic bias of radiographs measuring a larger altered lateral center-edge angle than 3D CT was observed, which disproved the hypothesis that a high correlation would exist between measurements made using either imaging modality. Nevertheless, intermethod quantitative bias is not critical because it will remain relatively consistent between modalities as evidenced by the strong individual reproducibility of each measurement. This suggests that radiographs can be reliably used to determine and classify potentially pathologic measurements, regardless of strictly quantitative differences between angles and distances measured via radiographs and 3D CT.

The results of the present study indicate the altered lateral center-edge angle could aid in screening for lateral morphological changes to the AIIS in clinical settings, whereas the altered anterior center-edge angle could detect anterior or inferior morphological changes. For example, with inferior morphology changes to the AIIS (as expected in subspinal impingement), the angle determined by the altered anterior center-edge angle measurement would be expected to increase. In addition, the appropriate amount of intraoperative AIIS decompression could be readily determined if a population mean distance from the 12 o'clock position on the acetabular rim to the AIIS was known.

The AIIS has been gaining attention as an extra-articular hip landmark due to its involvement in hip pathologies related to altered bony morphology (e.g., subspinal impingements) and tendon attachment (e.g., avulsions and calcific tendinitis). Previous studies have reported on the morphology of the AIIS as it relates to the normal population[15] and subspinal impingements.[9] Amar et al.[15] studied 50 patients and developed measurements related to the AIIS using 2D CT to describe the size, location, and position of AIIS with respect to patient size and sex. However, their measurements did not address the radiographic or 3D CT appearance of the AIIS in these situations. Hetsroni et al.[9] retrospectively studied 53 patients with symptomatic FAI. By evaluating the AIIS for subspinal impingement, they were able to develop a qualitative method for describing AIIS morphology, but did not relate their findings to radiographs.

The present study focused on developing reproducible measurements related to the AIIS relevant for radiographs or 3D CT images and, therefore, provided both quantitative values and corresponding insights into the measurement differences between the 2 imaging modalities. These newly proposed quantitative measurements could aid in the preoperative and postoperative evaluation of patients with subspinal impingement caused by the AIIS, while also reducing radiation exposure when compared with CT examination. The results of this study provide additional radiographic precision to the work presented by Lee et al.[16] by providing a medial to lateral approximation of the location of the AIIS on AP radiographs. In addition, the results of this study add to the work performed by Philippon et al.,[24] who reported on the anatomic distance from the stellate crease to the AIIS. Specifically, the measurements from the newly defined 12 o'clock position on the acetabular rim (located within 30 minutes of the stellate crease) to the AIIS on false-profile radiographs (41.4 ± 5.86 mm) and 3D CT (41.5 ± 3.60 mm) correlate well with the anatomic measurement from the AIIS to the stellate crease (38.4 ± 8.3 mm) reported in their study.[24]

In the future, using the methods proposed in this study, exact distance and angle measurements that define the morphology of the AIIS in symptomatic and asymptomatic subspinal impingement patient populations could be developed for both imaging modalities. These quantitative metrics could then be used in conjunction with the qualitative morphology classification developed by Hetsroni et al.[9] to better understand subspinal impingement. By extension, the distance measurement from the 12 o'clock position on the acetabular rim to the AIIS could also aid in determining the amount of AIIS to resect during operations. In addition, because there was a bias found between radiographs and 3D CT during the intermethod analysis, future studies could determine the level of clinical significance, or lack thereof, associated with the bias between the 2 modalities.

Limitations

The AP and false-profile views were standardized using an imaging platform to correctly orient each pelvis during radiographic imaging, eliminating a variable that exists within the clinical setting. However, limitations within the 3D modeling software required the CT scans to be oriented, using the ASIS and PSIS locations, within computational software. Thus, the assumption was made that these references on the iliac crests and the 2D orientation of the pelvis were not distinct from each other. Another limitation was the small number of specimens used for data collection. However, other anatomic studies have used similar specimen quantities.[25-28] Dissected cadaveric specimens with metallic spheres clearly defining the AIIS were used; however, the presence of soft tissue in living patients would not affect the defined measurements because bony landmarks, easily visible in radiographs and CT and unaffected by soft tissue, were referenced. In addition, in combination with the results from Lee et al.,[16] the quantitative location of the AIIS can now be more easily determined on AP and false-profile radiographs. Finally, because none of the cadaveric specimens exhibited a type 3 morphological AIIS variant as described by Hetsroni et al.,[9] it was not possible to

validate how measurement values would specifically change in this type of patient population.

Conclusions

AIIS morphology in relation to the acetabular rim 12 o'clock position and its angle relative to the sagittal plane can be quantitatively determined using either radiographic or 3D CT imaging modalities.

Acknowledgment

The authors thank Matthew T. Rasmussen, B.S., W. Andrew Lee, B.A., and Adriana J. Saroki, B.S., for their assistance with preparing specimens and acquiring radiographic and CT images.

References

1. Giordano BD, Grauer JN, Miller CP, Morgan TL, Rechtine GR II. Radiation exposure issues in orthopaedics. *J Bone Joint Surg Am* 2011;93:e69(1-10).
2. Weber AE, Jacobson JA, Bedi A. A review of imaging modalities for the hip. *Curr Rev Musculoskelet Med* 2013;6:226-234.
3. Nepple JJ, Martel JM, Kim YJ, Zaltz I, Clohisy JC. Do plain radiographs correlate with CT for imaging of cam-type femoroacetabular impingement? *Clin Orthop Relat Res* 2012;470:3313-3320.
4. Nepple JJ, Martell JM, Kim YJ, et al. Interobserver and intraobserver reliability of the radiographic analysis of femoroacetabular impingement and dysplasia using computer-assisted measurements. *Am J Sports Med* 2014;42:2393-2401.
5. Milone MT, Bedi A, Poultsides L, et al. Novel CT-based three-dimensional software improves the characterization of cam morphology. *Clin Orthop Relat Res* 2013;471:2484-2491.
6. Larson CM, Kelly BT, Stone RM. Making a case for anterior inferior iliac spine/subspine hip impingement: Three representative case reports and proposed concept. *Arthroscopy* 2011;27:1732-1737.
7. Zaltz I, Kelly BT, Hetsroni I, Bedi A. The crossover sign overestimates acetabular retroversion. *Clin Orthop Relat Res* 2013;471:2463-2470.
8. Hetsroni I, Larson CM, Dela Torre K, Zbeda RM, Magennis E, Kelly BT. Anterior inferior iliac spine deformity as an extra-articular source for hip impingement: A series of 10 patients treated with arthroscopic decompression. *Arthroscopy* 2012;28:1644-1653.
9. Hetsroni I, Poultsides L, Bedi A, Larson CM, Kelly BT. Anterior inferior iliac spine morphology correlates with hip range of motion: A classification system and dynamic model. *Clin Orthop Relat Res* 2013;471:2497-2503.
10. Reich MS, Shannon C, Tsai E, Salata MJ. Hip arthroscopy for extra-articular hip disease. *Curr Rev Musculoskelet Med* 2013;6:250-257.
11. Sutter R, Pfirrmann CW. Atypical hip impingement. *AJR Am J Roentgenol* 2013;201:W437-W442.
12. Pan H, Kawanabe K, Akiyama H, Goto K, Onishi E, Nakamura T. Operative treatment of hip impingement caused by hypertrophy of the anterior inferior iliac spine. *J Bone Joint Surg Br* 2008;90:677-679.
13. Schuett DJ, Bomar JD, Pennock AT. Pelvic apophyseal avulsion fractures: A retrospective review of 228 cases. *J Pediatr Orthop* 2015;35:617-623.
14. Peng X, Feng Y, Chen G, Yang L. Arthroscopic treatment of chronically painful calcific tendinitis of the rectus femoris. *Eur J Med Res* 2013;18:49.
15. Amar E, Druckmann I, Flusser G, Safran MR, Salai M, Rath E. The anterior inferior iliac spine: size, position, and location. An anthropometric and sex survey. *Arthroscopy* 2013;29:874-881.
16. Lee WA, Saroki AJ, Løken S, et al. Radiographic identification of arthroscopically relevant acetabular structures. *Am J Sports Med* 2016;44:67-73.
17. Lee WA, Saroki AJ, Løken S, et al. Radiographic identification of arthroscopically relevant proximal femoral structures. *Am J Sports Med* 2016;44:60-66.
18. Clohisy JC, Carlisle JC, Beaule PE, et al. A systematic approach to the plain radiographic evaluation of the young adult hip. *J Bone Joint Surg Am* 2008;90:47-66 (suppl 4).
19. Siebenrock KA, Kalbermatten DF, Ganz R. Effect of pelvic tilt on acetabular retroversion: A study of pelves from cadavers. *Clin Orthop Relat Res* 2003;407:241-248.
20. Tannast M, Siebenrock KA, Anderson SE. Femoroacetabular impingement: Radiographic diagnosis—what the radiologist should know. *AJR Am J Roentgenol* 2007;188:1540-1552.
21. Wu G, Siegler S, Allard P, et al. ISB recommendation on definitions of joint coordinate system of various joints for the reporting of human joint motion—part I: Ankle, hip, and spine. International Society of Biomechanics. *J Biomech* 2002;35:543-548.
22. Needell SD, Borzykowski RM, Carreira DS, Kozy J. CT false-profile view of the hip: A reproducible method of measuring anterior acetabular coverage using volume CT data. *Skeletal Radiol* 2014;43:1605-1611.
23. Fleiss J. *Statistical Methods for Rates and Proportions*, Ed 2. New York, NY: Wiley, 1981.
24. Philippon MJ, Michalski MP, Campbell KJ, et al. An anatomical study of the acetabulum with clinical applications to hip arthroscopy. *J Bone Joint Surg Am* 2014;96:1673-1682.
25. Haytmanek CT, Williams BT, James EW, et al. Radiographic identification of the primary lateral ankle structures. *Am J Sports Med* 2015;43:79-87.
26. James EW, LaPrade CM, Ellman MB, Wijdicks CA, Engebretsen L, LaPrade RF. Radiographic identification of the anterior and posterior root attachments of the medial and lateral menisci. *Am J Sports Med* 2014;42:2707-2714.
27. Johannsen AM, Anderson CJ, Wijdicks CA, Engebretsen L, LaPrade RF. Radiographic landmarks for tunnel positioning in posterior cruciate ligament reconstructions. *Am J Sports Med* 2013;41:35-42.
28. Pietrini SD, LaPrade RF, Griffith CJ, Wijdicks CA, Ziegler CG. Radiographic identification of the primary posterolateral knee structures. *Am J Sports Med* 2009;37:542-551.